

Assessment of intercomponent interaction in phenylene bridged dinuclear ruthenium(II) and osmium(II) polypyridyl complexes†

Adrian L. Guckian,^a Manfred Doering,^b Michael Ciesielski,^b Olaf Walter,^b Johan Hjelm,^a Noel M. O'Boyle,^a William Henry,^a Wesley R. Browne,^a John J. McGarvey^c and Johannes G. Vos^{*a}

^a National Centre for Sensor Research, School of Chemical Sciences, Dublin City University, Glasnevin, Dublin 9, Ireland. E-mail: han.vos@dcu.ie; Fax: 00353-1-7005503; Tel: 00353-1-7005307

^b ITC-CPV, Forschungszentrum Karlsruhe, PO Box 3640, 76021, Karlsruhe, Germany

^c School of Chemistry, Queen's University Belfast, Belfast, Northern Ireland, UK BT9 5AG

Received 16th June 2004, Accepted 11th October 2004

First published as an Advance Article on the web 3rd November 2004

The synthesis and characterisation of $[\text{Ru}(\text{bipy})_2(\text{L1})]^{2+}$ and the homodinuclear complexes $[\text{M}(\text{bipy})_2(\text{L1})\text{M}(\text{bipy})_2]^{4+}$ (where $\text{M} = \text{Ru}$ or Os), employing the ditopic ligand, 1,4-phenylene-bis(1-pyridin-2-ylimidazo[1,5-*a*]pyridine) (**L1**), are reported. The complexes are identified by elemental analysis, UV/Vis, emission, resonance Raman, transient resonance Raman and ^1H NMR spectroscopy, mass spectrometry and electrochemistry. The X-ray structure of the complex $[\text{Ru}(\text{bipy})_2(\text{L1})(\text{bipy})_2\text{Ru}](\text{PF}_6)_4$ is also reported. DFT calculations, carried out to model the electronic properties of the compounds, are in good agreement with experiment. Minimal communication between the metal centres is observed. The low level of ground state electronic interaction is rationalized in terms of the poor ability of the phenyl spacer in facilitating superexchange interactions. Using the electronic and electrochemical data a detailed picture of the electronic properties of the **RuRu** compound is presented.

Introduction

The design and synthesis of polynuclear transition metal complexes containing electro-active and photo-active units are topics of continuing interest due to their potential usage as building blocks for supramolecular assemblies and molecular devices.¹ Ruthenium(II) and osmium(II) polypyridine complexes are playing a key role in the development of compounds capable of performing photo- and/or redox-triggered useful functions in charge separation devices for photochemical solar energy conversion² and information storage.^{1,3} In particular, species featuring photophysical properties and redox behaviour, which can undergo controlled modification with external stimuli, are of interest.^{3,4} For example, reversible electrochemical switching of emission energy shows potential in applications such as electronic displays.⁵ The role played by the bridging ligand in determining intercomponent interaction is well recognised.^{6,7} Since the late 1970s, ground and excited state intercomponent interactions in dinuclear Ru(II) complexes containing polytopic bridging ligands employing imidazoles,⁸ triazoles,⁹ pyrazine,¹⁰ 4,4'-bipyridyl,¹¹ 2,2'-bipyrimidine,¹² tetrazine,¹³ have received considerable attention. The incorporation of spacer units (*i.e.*, phenylene,¹⁴ dimethoxyphenyl,¹⁶ thienyl,^{9c} *etc.*) has allowed for further control over the degree of interaction between metal centres in multinuclear complexes.

In this contribution the structural, photophysical and electrochemical characterisation of two symmetrical, phenylene bridged complexes of the form $[\text{M}(\text{bipy})_2(\text{L1})\text{M}(\text{bipy})_2](\text{PF}_6)_4$ (where $\text{M} = \text{Ru}(\text{II})$ or $\text{Os}(\text{II})$ and **L1** = 1,4-phenylene-bis(1-pyridin-2-ylimidazo[1,5-*a*]pyridine)) are reported (see Fig. 1). Selective deuteration is employed to facilitate interpretation of

^1H NMR, luminescence and resonance Raman spectra. DFT calculations are described for **RuRu**. A detailed description of the electronic properties of this compound is presented based on these calculations and the results obtained are compared with experimental data. Furthermore, the results obtained are discussed in the context of earlier studies on related complexes.

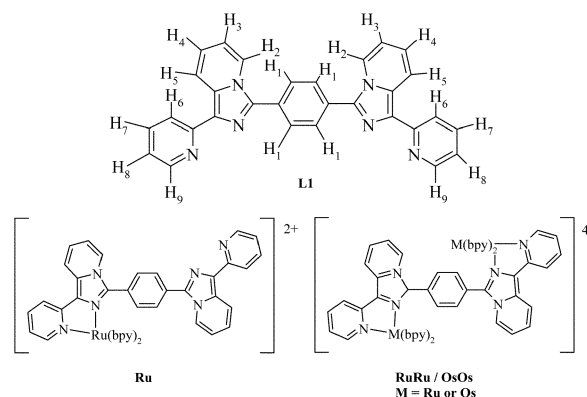


Fig. 1 Structure of the mononuclear and dinuclear complexes and **L1**.

Experimental

All reagents were of HPLC grade or better and used as received. Spectroscopic grade (UVASOL) solvents were employed for all spectroscopic measurements. d_8 -2,2'-bipyridyl (d_8 -bipy) (Complex Solutions, Dublin, Ireland) was used as received, *cis*- $[\text{Ru}(\text{bipy})_2\text{Cl}_2]\cdot 2\text{H}_2\text{O}$, its deuteriated analogue *cis*- $[\text{Ru}(d_8\text{-bipy})_2\text{Cl}_2]\cdot 2\text{H}_2\text{O}$ ¹⁵ and *cis*- $[\text{Os}(\text{bipy})_2\text{Cl}_2]\cdot 2\text{H}_2\text{O}$ ¹⁶ were prepared by previously reported procedures.

Syntheses

$[\text{Ru}(\text{bipy})_2(\text{L1})](\text{PF}_6)_2\cdot 2\text{H}_2\text{O}$ (Ru**).** **L1** (102 mg, 0.219 mmol) was heated at reflux in 300 cm³ of a 1 : 1 EtOH/H₂O mixture. *cis*- $[\text{Ru}(\text{bipy})_2\text{Cl}_2]\cdot 2\text{H}_2\text{O}$ (114 mg, 0.219 mmol) in 20 cm³ EtOH

† Electronic supplementary information (ESI) available: Fig. S1: ^1H NMR spectra of **Ru** and **RuRu**. Fig. S2: Resonance Raman spectra of **dRuRu**, **RuRu** and **OsOs**. Fig. S3: Reductive and oxidative electrochemistry of **Ru**. Fig. S4: Frontier orbitals of **RuRu**. Table S1: ^1H NMR spectra of **L1** and **L1** in **dRuRu**. Table S2: Selected bond distances. Table S3: Selected bond angles. Table S4: Calculated data for the frontier orbitals of **RuRu**. See <http://www.rsc.org/suppdata/dt/b4/b409189b/>

was added over 90 min. After 3 h the reaction was allowed to cool and the volume reduced *in vacuo*. The solution was filtered to remove unreacted ligand. 10 cm³ of a saturated aqueous solution of ammonium hexafluorophosphate was added to the filtrate yielding an orange–brown precipitate, which was isolated by filtration, washed with 25 cm³ of water, 25 cm³ of diethyl ether and air-dried. The compound was purified by column chromatography (silica gel, 0.05 M KNO₃ acetonitrile–water (80/20 v/v)). The first orange band eluted, yielded the desired product. The acetonitrile was removed *in vacuo* and an excess of NH₄PF₆ added to precipitate the product. The precipitate was filtered, washed with 25 cm³ cold water and 25 cm³ diethyl ether. Yield 95 mg (37%). Mass spectrometry: *m/z* calculated for [Ru](PF₆)₃⁺: 1023.2. Found: 1023.3. ¹H NMR spectrum (400 MHz, *d*₆-DMSO) δ 6.95 (dd, 1H), 7.24 (m, 4H), 7.44 (m, 2H), 7.60 (m, 7H), 7.78 (d, 1H), 7.82 (d, 1H), 7.88 (m, 2H), 7.97 (d, 1H), 8.14 (m, 7H), 8.29 (d, 1H), 8.53 (m, 5H), 8.66 (d, 1H), 8.74 (m, 3H). Elemental analysis for C₃₀H₄₀N₁₀Ru₁O₂P₂F₁₂: Calc.: C 50.04, H 3.17, N 11.68. Found C 49.45, H 3.01, N 11.19%.

[Ru(bipy)₂(L1)Ru(bipy)₂(PF₆)₄·4H₂O (RuRu)]. L1 (200 mg, 0.43 mmol) and *cis*-[Ru(bipy)₂Cl₂]·2H₂O (492 mg, 0.946 mmol) were heated at reflux in 30 cm³ (1 : 1) EtOH–H₂O for 16 h. The solution was cooled to r.t., reduced *in vacuo* and filtered to remove unreacted ligand. 5 cm³ of a saturated aqueous solution of ammonium hexafluorophosphate was added to the filtrate to yield an orange–brown precipitate, which was filtered off, washed with 25 cm³ water and 25 cm³ diethyl ether. The compound was purified by column chromatography (as for Ru). The second orange band to elute yielded the desired product. Yield 650 mg (81%). Mass spectrometry: *m/z* calculated for [RuRu](PF₆)₃⁺: 1727.15. Found: 1727.3. ¹H NMR spectrum (400 MHz, *d*₆-DMSO) δ 6.75 (dd, 1H), 6.94 (dd, 1H), 7.24 (m, 8H), 7.43 (m, 7H), 7.60 (m, 10H), 7.80 (d, 1H), 7.90 (d, 1H), 8.16 (m, 12H), 8.40 (d, 1H), 8.63 (m, 6H), 8.75 (m, 4H). Elemental analysis for C₇₀H₆₀N₁₄Ru₂O₄P₄F₂₄: Calc.: C 43.43, H 2.90, N 10.13. Found: C 43.11, H 3.08, N 10.01%.

[Ru(*d*₈-bipy)₂(L1)Ru(*d*₈-bipy)₂(PF₆)₄·4H₂O (*d*RuRu)]. As for RuRu except L1 (50 mg, 0.107 mmol) and *cis*-[Ru(*d*₈-bipy)₂Cl₂]·2H₂O (127 mg, 0.237 mmol) were heated at reflux in 20 cm³ of 1 : 1 EtOH–H₂O. Yield 112 mg (55%). Mass spectrometry: *m/z* calculated for [*d*RuRu](PF₆)₃⁺: 1759.2. Found: 1758.3 [M⁺]. ¹H NMR spectrum (400 MHz, *d*₆-DMSO) δ 7.27 (m, 3H), 7.41 (d, 2H), 7.60 (m, 2H), 8.05 (dd, 1H), 8.63 (m, 2H). Elemental analysis for C₇₀H₂₈N₁₄D₃₂Ru₂O₄P₄F₂₄: Calc.: C 42.73, H 2.85, N 9.97. Found C 43.21, H 2.98, N 9.51%.

[Os(bipy)₂(L1)Os(bipy)₂(PF₆)₄·4H₂O (OsOs)]. As for RuRu except L1 (200 mg, 0.43 mmol) and *cis*-[Os(bipy)₂Cl₂]·2H₂O (523 mg, 0.946 mmol) were heated at reflux in 20 cm³ of 1 : 1 ethylene glycol–H₂O for 72 h. Yield 549 mg (62%). Mass spectrometry: *m/z* calculated for [OsOs](PF₆)₃⁺: 1907.3. Found: 1908.1 [M⁺]. ¹H NMR spectrum (400 MHz, *d*₆-acetone) δ 6.81 (dd, 2H), 7.06 (dd, 1H), 7.25 (m, 7H), 7.53 (m, 13H), 7.74 (d, 1H), 7.94 (m, 14H), 8.26 (d, 1H), 8.40 (d, 1H), 8.46 (m, 2H), 8.65 (m, 10H). Elemental analysis for C₇₀H₆₀N₁₄Os₂O₄P₄F₂₄: Calc.: C 39.77, H 2.65, N 9.28. Found C 39.44, H 2.39, N 9.41%.

X-Ray crystallography

Data for RuRu were collected on a Siemens SMART 1000 CCD-diffractometer fitted with a molybdenum tube (Mo-Kα, λ = 0.71073 Å) and a graphite monochromator. A full sphere of data was collected with the irradiation time of 4 s per frame. The structures were solved with direct methods and all non hydrogen atoms refined anisotropically with the SHELX-97 program¹⁷ (refinement by least-squares against F²). *Crystal data*: RuRu: [Ru(bipy)₂(L1)Ru(bipy)₂(PF₆)₄], C_{75.1}H₅₂F₂₄N₁₄P₄O_{1.7}Ru₂; M_r = 1959.73; monoclinic, P2₁/c, a = 15.0193(15), b = 24.332(3), c = 21.810(2) Å, β = 96.956(2), V = 7911.9 Å³; D_c = 1.645 Mg m⁻³, data collection range: h –20 to 19, k = –30 to 32, l = –26 to 28;

reflections collected: 85840, reflections unique: 19449, reflections observed (I > 2σI): 8985, final R-values: R1 = 0.054 (I > 2σI), wR2 = 0.156 (all data).

CCDC reference number 230287.

See <http://www.rsc.org/suppdata/dt/b4/b409189b/> for crystallographic data in CIF or other electronic format.

Physical methods

¹H NMR spectra were recorded on a Bruker Avance 400 (400 MHz) instrument. The chemical shifts are relative to residual solvent peaks. UV/Visible spectra were recorded using a Shimadzu UV3100 UV-Vis-NIR spectrophotometer interfaced with an Elonex PC433 personal computer (Molar absorptivities (ε) ±5%). Emission spectra were recorded on a Perkin-Elmer LS50-B spectrofluorimeter equipped with a red-sensitive Hamamatsu R928 detector, interfaced to an Elonex PC466 personal computer employing Perkin Elmer FL Winlab custom built software. Excitation and emission slit widths were 10 nm. The spectra are not corrected for photo multiplier response. Luminescence lifetime measurements were obtained using an Edinburgh Analytical Instruments Time Correlated Single Photon Counting apparatus.^{9a} Excitation employed the 337 nm N₂ emission line of the nanosecond flashlamp. Cyclic voltammetry (100 mV s⁻¹) and DPV (step height: 50 mV, increment: 4 mV, pulse duration: 60 ms, sampling interval: 20 ms, frequency: 5 Hz) were carried out in acetonitrile with 0.1 M TBABF₄. A conventional three-electrode cell was used. A 2 mm Pt disk electrode sealed in Kel-F (purchased from CH Instruments) was used as the working electrode, the counter (auxiliary) electrode was a coiled Pt-wire, and a Ag/Ag⁺ (10 mM AgNO₃, 0.1 M TBABF₄ in acetonitrile) half-cell was used as reference electrode. The solutions were deoxygenated with argon and a blanket of argon was maintained over the solutions during the experiments. Glassware used was dried in a vacuum oven at 80 °C overnight or flamed using a Bunsen burner prior to preparing solutions. The TBABF₄ salt was dried in the vacuum oven overnight at 80 °C. The electrodes were polished on a soft polishing pad (Struers, OP-NAP) with an aqueous slurry of 0.3 micron alumina (Buehler) and sonicated for at least 5 min in MQ-water to remove any remaining polishing material from the surface of the electrode. The working electrodes were rinsed thoroughly with acetone and dried in air before insertion into the cell. The reference electrode was calibrated externally by carrying out cyclic voltammetry (also at 100 mV s⁻¹) in solutions of ferrocene of similar concentration as that of the complexes (0.4–2 mM) in the same electrolyte at the end of each day of experiments. Bulk electrolysis was carried out in a three-compartment, three-electrode cell. The reference electrode was Ag/Ag⁺, the working electrode was a cylinder of Pt gauze, 1 cm × 1 cm (52 mesh) and the counter electrode used was a coiled Pt wire. Spectroelectrochemistry¹⁸ was carried out in 0.1 M TEAP acetonitrile (anhydrous, Aldrich). The potential was controlled using a EG&G PARC Model 362 scanning potentiostat. A platinum/rhodium gauze working electrode, Ag/Ag⁺ reference electrode (calibrated against the Fc/Fc⁺ standard prior to each experiment) and platinum wire counter electrode was employed. All references are quoted relative to Fc/Fc⁺ using the relevant conversion factor.^{19,20} Absorption spectra of the species generated in the optically transparent thin layer electrode (OTTLE) cell were recorded on a Shimadzu 3100 UV-Vis/NIR spectrophotometer (*vide supra*). Elemental analysis was carried out by the Microanalytical Laboratories at University College Dublin.

Ground-state resonance Raman spectra of the complexes were recorded at 457.9, 488 and 514 nm using an argon ion laser (Spectra Physics model 2050) as the excitation source.²¹ The laser power at the sample was typically 30–40 mW. The Raman backscatter was focused onto the entrance slit of a single stage spectrograph (JY Horiba HR640), which was coupled to a CCD

detector (Andor Technology DV420-OE). The spectra were run in quartz cuvettes and were not corrected for detector response. Transient resonance Raman spectra were recorded using the single-colour pump and probe method in which the leading edge of the pulse excites the molecules and the trailing edge probes the resultant Raman scattering.²² The excitation source was a pulsed laser (Spectra Physics Q-switched Nd:YAG, GCR-3) at 354.7 nm with a typical pulse energy of approx. 3 mJ at the sample. The Raman backscatter was focused onto the entrance slit of a double-stage spectrograph (Spex 1870), which was coupled to an ICCD (Andor Technology DH501). Typically, spectra were collected as a summation of 6000 accumulations.

Density functional theory (DFT) calculations were carried out using Gaussian03.²³ Becke's 3-parameter hybrid functional²⁴ was used with the correlation functional of Lee, Yang and Parr²⁵ (B3LYP). The effective core potential basis set LanL2DZ²⁶ was used for all atoms. Although the crystallographic structure of the dimer was of C_1 symmetry, due to the size of the system it was necessary to reduce the computational cost by imposing C_2 symmetry during the geometry optimisation. The homochiral $\Delta\Delta$ isomer was studied. The resulting electronic structure is not expected to differ significantly for the other stereoisomers. GaussSum²⁷ was used to calculate the contributions from groups of atoms to each molecular orbital and to convolute the molecular orbital data to create a partial density of states (PDOS) spectrum. The contributions were calculated within the framework of a Mulliken population analysis. The PDOS was convoluted with Gaussian curves of FWHM of 0.3 eV and unit height.

Results and discussion

The very low solubility of **L1** in comparison with the mononuclear complex (**Ru**) results in the rapid formation of the binuclear complex once the mononuclear complex forms. To overcome this, **Ru** was prepared by slow addition of *cis*-[Ru(bipy)₂Cl₂] to a large volume of solvent saturated with **L1**, heated at reflux. **RuRu** and **OsOs** were prepared by direct reaction of two equivalents of *cis*-[M(bipy)₂Cl₂] (where M = Ru(II) or Os(II)) with one equivalent of **L1** in ethanol–water and ethylene glycol–water, respectively.

X-Ray crystallography

The molecular structure of **RuRu** is shown in Fig. 2. Selected bond angles and lengths are listed in Tables S1 and S2 (ESI†). **RuRu** co-crystallized with 1.7 molecules of acetone per unit cell and four hexafluorophosphate counter anions, (three of which are disordered). From the crystal structure it is clear

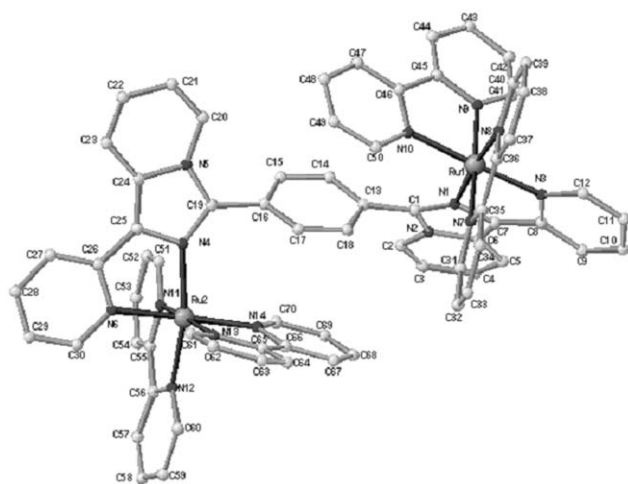


Fig. 2 X-Ray crystal structure of **RuRu** showing the atomic numbering used. The PF₆⁻ ions, acetone molecules and hydrogen atoms have been omitted for clarity.

that **L1** is coordinated to Ru1 *via* the N1 and N3 atoms and the Ru2 atom *via* the N4 and N6 atoms. The bite angle of the N(1)–Ru(1)–N(3) is 78.65(16)° and N(4)–Ru(2)–N(6) is 78.63(16)° which corresponds well with the bite angle of 77.9(1)° obtained by Hage *et al.* for [Ru(bipy)₂(3-(2-hydroxyphenyl)-5-(pyridin-2-yl)-1,2,4-triazole)]PF₆·CH₃COCH₃.²⁸ Bite angles of between 79.35(16) and 78.86(17)° for bipyridine ligands and Ru–N distances of 2.045(4)–2.068(4) Å are also comparable to those found in other complexes.^{9,14,28} One factor contributing to the increased length of the Ru(1)–N(1) and Ru(2)–N(4) bond lengths (2.080(4) and 2.086(4) Å, respectively) is the limited π -backbonding to the electron rich bridging ligand from the metal centre. The N1–Ru1–N8, N3–Ru1–N10 and N7–Ru1–N9 angles are 174.81(15), 175.85(16) and 176.44(16)°, respectively, while the *trans* angular bond angles around the Ru2 atom are 169.22(16), 175.74(16) and 172.83(17)° for N4–Ru2–N12, N6–Ru2–N14 and N11–Ru2–N13, respectively. This deviation from octahedral geometry is due to the acute bite angles of both the 2,2'-bipyridyl and the **L1** ligand. The internuclear (Ru...Ru) separation is 9.06 Å and the orientation of the phenyl ring of **L1** is distorted from planarity (by 61.1°) with respect to the imidazole rings.

¹H NMR Spectroscopy

The ¹H NMR spectroscopic data of all the complexes are given in the Experimental section (see Table S3 and Fig. S1, ESI†). As expected the protons of the **L1** ligand are shifted downfield upon coordination. The symmetry of **L1** is retained upon addition of the two equivalent metal centres, which greatly simplifies the spectra of the homonuclear (**RuRu** and **OsOs**) complexes.²⁹ Deuteration of the bipy ligands allowed for the identification of the **L1** protons in the **dRuRu** complex.³⁰

Electronic and photophysical properties

The absorption spectra of **Ru** and **RuRu** are similar, differing only in that the molar absorptivity of the dinuclear compound is almost twice that of the mononuclear complex (Table 1). The electronic data of **L1** are shown in Fig. 3(c). The ligand shows a number of features in the visible part of the spectrum, with absorption maxima at 277, 330 and 372 nm. At room temperature an emission is observed at 455 nm. The UV/Vis absorption spectra of the complexes (Fig. 3) are reminiscent with those observed for related Ru(II) and Os(II) imidazole and benzimidazole based complexes reported by Haga and co-workers.⁸ The visible region of the spectra is dominated by $d\pi \rightarrow \pi^*$ MLCT transitions, while $\pi \rightarrow \pi^*$ (bipy) and $\pi \rightarrow \pi^*$ (**L1**) transitions are located at *ca.* 290 and 350 nm, respectively (*vide infra*). The metal-to-ligand-charge-transfer (¹MLCT) bands for the Ru(II) complexes are close in energy to the transition observed for [Ru(bipy)₃]²⁺ and are assigned as $d\pi \rightarrow \pi_{\text{bipy}}^*$ ¹MLCT, based on electrochemical and resonance Raman data (*vide infra*). In the mixed-metal complex, **OsOs**, absorption bands between 580 and 700 nm are assigned to formally spin forbidden $d\pi \rightarrow \pi^*$ (bipy) (³MLCT) transitions. Comparison of the spectroscopic properties of the binuclear complexes with the parent [M(bipy)₃]²⁺ (where M = Ru or Os) indicates that transitions involving the bridging ligand **L1** are responsible for the absorption features at around 350 nm. The nature of this band is further discussed in the resonance Raman section.

All compounds are luminescent in acetonitrile at room temperature and in butyronitrile glass at 77 K. As for the absorption spectra only a modest (~15 nm) red shift in the emission spectrum with respect to [M(bipy)₃]²⁺ (M = Ru or Os) is observed (Table 1) and, typical of ³MLCT emission, the emission undergoes a blue shift on cooling to 77 K.³¹ The luminescence lifetimes of **Ru** (690 ns) and **RuRu** (506 ns) in deaerated acetonitrile are comparable to the luminescence lifetimes of related complexes (*e.g.*, benzimidazoles, triazoles *etc.*).^{8,32} Deuteration of the bipyridyl ligands leads to an increase

Table 1 Photophysical and electrochemical data in CH₃CN

	Abs. $\lambda_{\text{max}}/\text{nm}$ ($10^{-4}\epsilon/\text{M}^{-1}\text{cm}^{-1}$) ^a	Lum. $\lambda_{\text{max}}/\text{nm}$ 298 K (τ/ns) ^b	Lum. $\lambda_{\text{max}}/\text{nm}$ 77 K ($\tau/\mu\text{s}$) ^b	Oxid. ^c /V	Red. ^c /V
Ru	290 (7.73), 365 (3.67), 454 (1.135)	628 (690)	598	0.79, 1.42 <i>irr</i> ^d	-1.78, -2.01
RuRu	290 (12.97), 357 (4.62), 457 (1.95)	625 (506)	602	0.79, 1.41 <i>irr</i> ^d	-1.76, -2.03
dRu/Ru		625 (940)	602		
OsOs	293 (13.5), 359 (4.73), 484 (1.79), 624 (0.72)	753 (39)	738	0.36, 1.41 <i>irr</i> ^d	-1.77, -1.99
[Ru(bipy) ₃] ²⁺ ^e	452	620 (1000)	590 (5100)	0.88	-1.82, -2.01, -2.26
[Os(bipy) ₃] ²⁺ ^f	640	723 (62)	940	0.45	-1.65

^a In CH₃CN. ^b In butyronitrile. ^c vs. Fc/Fc⁺. ^d Ligand oxidations are sensitive to conditions. ^e Ref. 36. ^f Ref. 37.

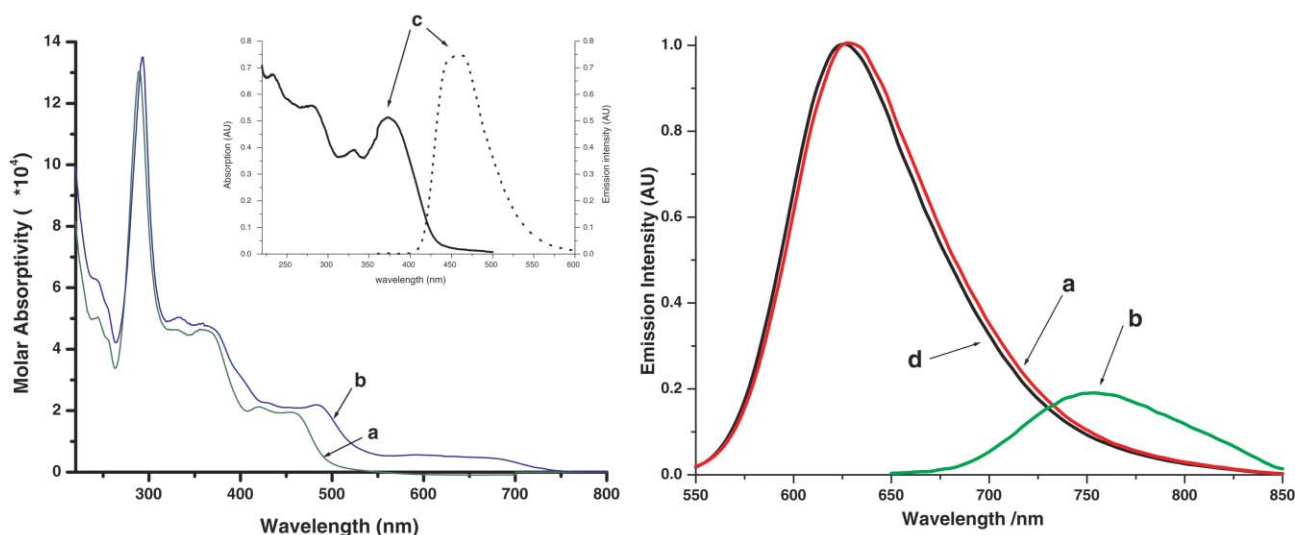


Fig. 3 Absorption (left) and emission (right) spectra in acetonitrile: (a) **RuRu**, (b) **OsOs** and (d) **Ru** [inset: absorption and emission spectra of (c) **L1**].

in the emission lifetime of the **RuRu** complex from 506 to 940 ns (185%), suggesting that the lowest emissive excited state is ³MLCT(bipy) in nature and not ³MLCT(L1).³³

Resonance Raman and transient Resonance Raman spectroscopy

Resonance Raman (rR) spectroscopy enables the assignment of the optical transitions in the visible region of the absorption spectrum. Using excitation wavelengths coincident with absorption bands results in resonant enhancement of vibrational modes of the chromophore by several orders of magnitude. This allows for assignment of optical transitions. The ground and excited state rR spectra of the **L1** based complexes are complicated by the overlap of resonant chromophores in the visible region, e.g. the $M(d\pi)$ or $L1(\pi) \rightarrow L1(\pi^*)$ and $M(d\pi) \rightarrow \text{bipy}(\pi^*)$ MLCT transitions. In the case of the Os(II) based complexes the spectra are further complicated by the presence of formally spin forbidden ³MLCT transitions. Resonance Raman spectra recorded at 457.9 and 488 nm excitation for all complexes reveal only vibrational modes associated with $M(d\pi) \rightarrow \text{bipy}(\pi^*)$ ¹MLCT absorption bands, this conclusion is confirmed by isotopic shift observed for **dRu/Ru**, as shown in Fig. S2, ESI.† It would be anticipated therefore that emission is ³MLCT(bipy) based, an assignment supported by the observation that, upon deuteration of the bipy ligands, the emission lifetime observed almost doubles.

Excited state (or transient) resonance Raman spectroscopy (TR²) proves to be an invaluable tool in confirming the nature of the emissive ³MLCT state. The observation of features characteristic of bipy^{-*} anion radical (i.e. bands at 1212 and 1285 cm⁻¹) in the TR² spectrum at 354.67 nm excitation, indicate a bipy-based ³MLCT excited state is present.³⁴ However, as shown in Fig. 4 the presence of a strong **L1** based transition at 350 nm complicates

the transient rR spectrum obtained at 354.5 nm excitation, with **L1** ligand modes being observed. The presence of vibrational features due to **L1** raises the possibility that the bands at 1212 and 1285 cm⁻¹ are **L1** bands. It is in assigning vibrational modes that deuteration becomes invaluable. Upon deuteration the principle marker bands for bipy^{-*} (1212 and 1285 cm⁻¹) disappear and a feature at 1186 cm⁻¹ tentatively assigned to *d*₈-bipy^{-*} is observed (the 1334 cm⁻¹ band of *d*₈-bipy^{-*} is masked by **L1** vibrations), confirming that these bands are bipy based. Since the **L1** based 350 nm absorption is independent of the nature of the metal, it has been assigned as an interligand $\pi-\pi^*$ transition.

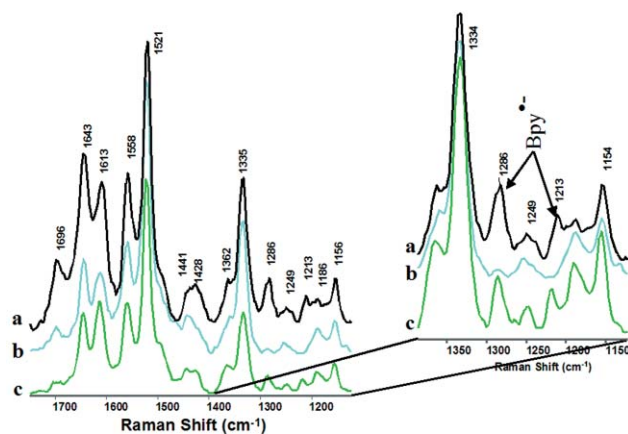


Fig. 4 TR² spectra at 354.67 nm of (a) **RuRu**, (b) **dRu/Ru** and (c) **OsOs** in H₂O-acetone (95/5 v/v) (spectra normalized to the 1521 cm⁻¹ band).

These results demonstrate that excitation of the complexes results in vibrational features which can be assigned to excited state bipy, and hence support the assignment of the lowest emitting $^3\text{MLCT}$ state as being bipy based.

Electrochemical properties

The oxidation and reduction potentials of **Ru**, **RuRu** and **OsOs** are presented in Table 1, differential pulse and cyclic voltammograms for the dinuclear complexes are shown in Fig. 5 (for **Ru** see Fig. S3, ESI†). The assignment of the oxidation processes observed is not straightforward due to the presence of the **L1** ligand, which undergoes irreversible oxidation. Assignment of the metal based redox processes is, however, possible by comparison with $[\text{Ru}(\text{bipy})_3]^{2+}$ and $[\text{Os}(\text{bipy})_3]^{2+}$. The fact that **L1** is oxidised at relatively low anodic potentials suggests that it is electron rich and is supported by the DFT calculations (*vide infra*). The **OsOs** complex displays a single oxidation wave at 0.36 V vs. Fc/Fc^+ which is 90 mV lower than that observed for $[\text{Os}(\text{bipy})_3]^{2+}$. The stabilisation of the Os(III) oxidation state in this compound with respect to $[\text{Os}(\text{bipy})_3]^{2+}$ is indicative of the presence of a stronger electron donating ligand (relative to bipy) in the inner coordination sphere of the Os ion. Similarly, for **Ru** and **RuRu** the metal redox potentials are 90 mV more cathodic than $[\text{Ru}(\text{bipy})_3]^{2+}$. The two equivalent Os centres undergo simultaneous one electron oxidations which indicates that any metal–metal interactions are relatively weak. This is further supported by the absence of mixed valence charge transfer transitions (*vide infra*). Attempts to resolve the metal centred redox wave of the **OsOs** compound using differential pulse voltammetry were unsuccessful (Fig. 5). The value of $n = 1.92$ determined by bulk electrolysis carried out on the **OsOs** compound confirms the bielectronic nature of the first oxidation wave. **RuRu** behaves similarly with a single metal oxidation wave being observed at 0.79 V and an irreversible feature at 1.42 V. The absence of separation between the first and second metal oxidation steps in the dinuclear complexes, is in agreement with other systems of similar internuclear separation and is due to the minimal electrostatic interactions observed over these distances.^{9c,35}

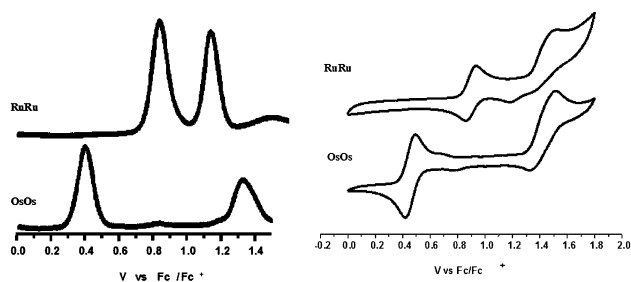


Fig. 5 DPV (left) and cyclic voltammograms (right) of **OsOs** and **RuRu** vs. Fc/Fc^+ with 0.1 M TBABF_4 in CH_3CN .

Based on the difference in formal potential of $[\text{Ru}(\text{bipy})_3]^{2+}$ and $[\text{Os}(\text{bipy})_3]^{2+}$, a potential difference of *ca.* 430 mV is expected between analogous Ru and Os metal centres. This compares well with the observed potential difference for the compounds reported of 430 mV.^{36,37} The irreversible processes observed at more anodic potentials are attributed to oxidation of the bridging **L1** ligand. These redox processes are ill defined and their potential is very dependent on the conditions employed, with variation in the anodic potentials of up to 200 mV being observed. The reasons for this are at present not fully understood. The reduction potentials are as expected and are in agreement with a bipy based LUMO.

Spectroelectrochemistry

Electrochemical studies discussed above indicate that for **RuRu** and **OsOs** communication between the metal centres in the

ground state is, at best, weak (comproportionation constant, $K_c \sim 4$).³⁸ To gain a better understanding of the true strength of the delocalisation of the SOMO in the mixed valence complex ($\text{M}^{\text{II}}\text{M}^{\text{III}}$) and hence internuclear communication, the spectroscopic properties of mixed valence dinuclear complexes were investigated. For the homonuclear complexes the single bielectronic metal oxidation process makes generation of the mixed valence species more difficult. Nevertheless spectroelectrochemistry has proven useful in determining the degree of intercomponent interaction in related dinuclear systems exhibiting single bielectronic metal redox processes.³⁵ A typical example of such spectroelectrochemical studies is shown in Fig. 6 for the compound **RuRu**. For the dinuclear complexes reversible spectral changes were observed at potentials below 1 V, however, bulk electrolysis at higher potentials results in irreversible spectral changes, which were not investigated further. Oxidation at 0.7 V vs. Fc/Fc^+ results in a gradual disappearance of the MLCT bands and a decrease in the intensity and red-shift in the $\pi \rightarrow \pi^*$ transition around 280 nm. Bleaching of the MLCT band continues at potentials higher than 0.7 V vs. Fc/Fc^+ . At these potentials a concurrent increase in the intensity of band in the region 500 to 800 nm, which can be expected to be ligand-to-metal-charge-transfer (LMCT) in nature. Importantly, neither complex show any evidence for the presence of an intervalence band in the mixed valence state, indicating little or no communication between the two metal centres in the ground state.

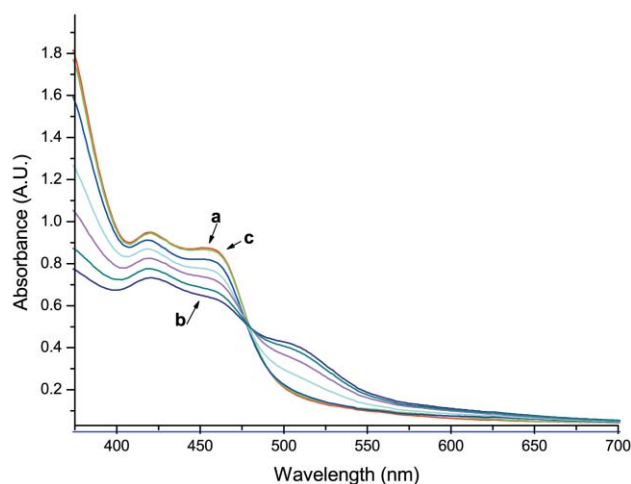


Fig. 6 Spectroelectrochemistry of the mixed metal complex **RuRu** in MeCN with 0.1 M TEAP at intervals from (a) 0 V to (b) 0.9 V and (c) after re-reduction at 0 V vs. Fc/Fc^+

DFT Calculations

The geometry optimisation of the dimer gave results in good agreement with the crystal structure. B3LYP has a tendency to overestimate the Ru–N bond length³⁹ (typically by 0.05 Å for the Ru– N_{bipy} bonds). From crystallographic data (*vide supra*) it is seen that for **RuRu** the Ru– N_{py} bond is longer than the Ru– N_{imid} bond (see Table S2, ESI†) but in the calculated structure the reverse is found (with the Ru– N_{imid} bond overestimated by 0.07 Å). The distortion from planarity of the phenyl ring with respect to the imidazole rings is reproduced by the calculations, although the dihedral angle is also overestimated by 7°. The calculated energies of the frontier orbitals are shown in Table S4 (ESI†). Each molecular orbital has been broken down in terms of a percentage contribution from the metal centres, *Ru*, the bipyridine ligands, *bipy*, the central phenyl ring of the **L1** ligand, *L1-ph*, and a moiety comprising the pyridine and fused rings of the **L1** ligand, *L1-py*. These data have been plotted in the form of a PDOS spectra in Fig. 7.⁴⁰

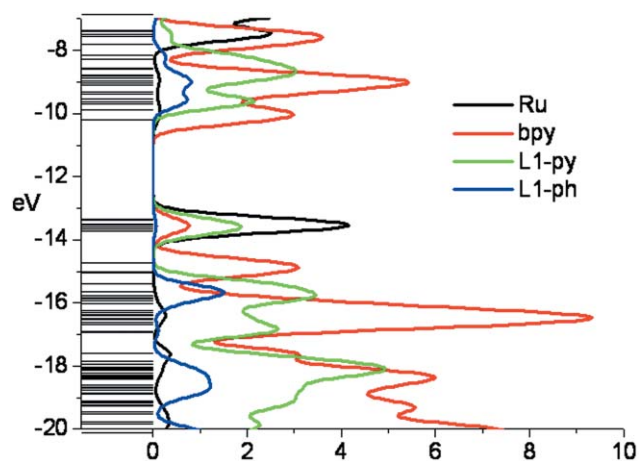


Fig. 7 Partial density of states (PDOS) spectrum of **RuRu** showing the percentage contributions of *Ru*, *bpy*, *L1-py* and *L1-ph* (see text) to the molecular orbitals.

The highest occupied metal orbitals are largely metal-based, but also contain a significant contribution from *L1-py* (See Fig. 8 and Table S4, ESI†). This agrees with the electrochemical results, which show that the first oxidation is metal-based but that oxidation of the ligand **L1** is also expected. The lowest unoccupied metal orbitals are bipyridine-based (see Fig. 8).

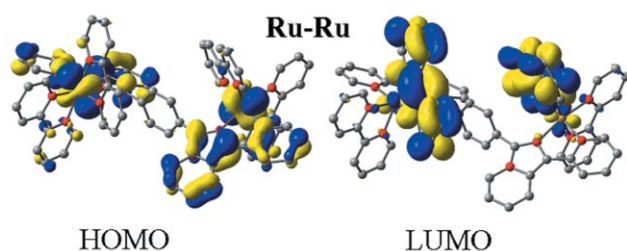


Fig. 8 Calculated HOMO and LUMO orbitals for **RuRu**.

Based on these ground state results, it is expected that the first reduction is *bpy*-based. It is worth noting also that the two moieties of **L1** are at best only weakly electronically coupled: for example, *L1-ph* does not contribute to the HOMO, in contrast to *L1-py*. This suggests that delocalisation of molecular orbitals across **L1** is unlikely to be significant.

A comparison of the molecular orbital data in Table S4 (and Fig. S4), ESI† and the energy level diagram of Fig. 9, which is based on the experimental results, shows some interesting parallels. The *bpy* $\pi \rightarrow \pi^*$ is reproduced using the ground state data (H-8 \rightarrow LUMO; 36000 cm^{-1}) although the energy of the **L1** $\pi \rightarrow \pi^*$ transition is overestimated (H-7 \rightarrow L+4; 32 000 cm^{-1}). The oxidation difference between **Ru** and **L1** can be estimated using the HOMO to H-7 distance as 2400 cm^{-1} , in good agreement with experiment. The HOMO \rightarrow LUMO distance (26000 cm^{-1}), on the other hand, does not agree with the experimental value. Accurate calculation of these values, including the inclusion of solvent was outside the scope of this experiment, but the estimates nevertheless give a satisfactory representation of the experimentally obtained parameters. The discrepancies observed are most likely due to the limitations of using ground state molecular orbital data to represent excited state systems, and to the fact that mixing of orbitals of the same symmetry has been neglected.

Conclusion

In the present study, intercomponent communication in dinuclear complexes is explored. Despite the relatively moderate internuclear separation, no detectable interaction between the metal centres is observed. It seems likely that the lack of

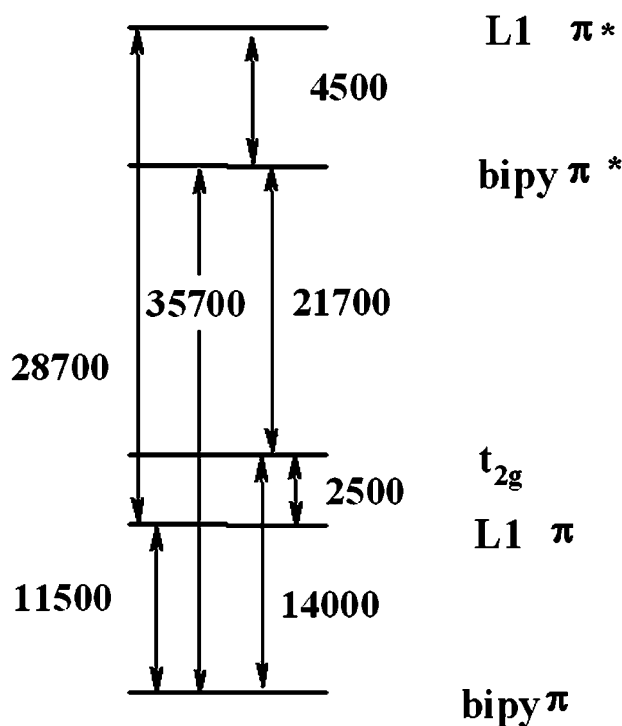


Fig. 9 Relative energy of energy levels in **RuRu**. Data used; *bpy* $\pi\pi^*$ 280 nm (35700 cm^{-1}); **L1** $\pi\pi^*$ 350 nm (28700 cm^{-1}). Lowest energy $^1\text{MLCT}$ 460 nm (21700 cm^{-1}); difference between oxidation of **Ru(II)** and **L1** is in 310 mV (2500 cm^{-1}).

communication can be rationalised by considering the inability of the phenyl ring to mediate such an interaction (both the X-ray data and the DFT calculations show that there is a significant deviation from planarity). In the absence of through-bond interaction, through-space interaction over the distance between to the $\text{M}(\text{bipy})_2$ moieties is likely to be very weak, however this in itself does not account for the absence of any excited state interaction. The location of the lowest excited $^3\text{MLCT}$ state on the peripheral *bpy* ligands and not on the bridging ligand increases the effective energy/electron transfer distance.

Acknowledgements

This work was partly supported by Enterprise Ireland (Grant Number SC/2003/74) and by the Improving Human Potential Programme (Grant Number HPRN-2002-00185).

References

- (a) L. A. Worl, G. F. Strouse, J. N. Younathan, S. M. Baxter and T. J. Meyer, *J. Am. Chem. Soc.*, 1990, **112**, 7571; (b) V. Balzani, *Tetrahedron*, 1992, **48**, 10443; (c) V. Balzani, S. Campagna, G. Denti, A. Juris, S. Serroni and M. Venturi, *Acc. Chem. Res.*, 1998, **31**, 26; (d) V. Balzani and F. Scandola, *Supramolecular Photochemistry*; Horwood, Chichester, UK, 1991; (e) F. Scandola, M. T. Indelli, C. Chiorboli and C. A. Bignozzi, *Top. Curr. Chem.*, 1990, **158**, 73.
- (a) K. Kalyanasundaram, *Coord. Chem. Rev.*, 1982, **46**, 159; (b) J.-M. Lehn, *Angew. Chem., Int. Ed. Engl.*, 1988, **27**, 89; (c) V. Balzani, S. Campagna, G. Denti, A. Juris and M. Ventura, *Coord. Chem. Rev.*, 1994, **132**, 1; (d) V. Balzani, A. Juris, M. Venturi, S. Campagna and S. Serroni, *Chem. Rev.*, 1996, **96**, 759; (e) C. A. Slate, D. R. Striplin, J. A. Moss, P. Chen, B. W. Erickson and T. J. Meyer, *J. Am. Chem. Soc.*, 1998, **120**, 4885; (f) Y.-Z. Hu, S. Tsukiji, S. Shinkai, S. Oishi and I. Hamachi, *J. Am. Chem. Soc.*, 2000, **122**, 241; (g) J.-P. Sauvage, J.-P. Collin, J.-C. Chambron, S. Guillerez, C. Coudret, V. Balzani, F. Barigelli, L. De Cola and L. Flamigni, *Chem. Rev.*, 1994, **94**, 993; (h) E. R. Carraway, J. N. Demas, B. A. DeGraff and J. R. Bacon, *Anal. Chem.*, 1991, **63**, 337.
- (a) *Supramolecular Photochemistry*, ed. V. Balzani, Reidel, Dordrecht, 1997; (b) J.-M. Lehn, *Supramolecular Chemistry*, Wiley-VCH, Weinheim, 1995.

- 4 (a) P. D. Beer, F. Szemes, V. Balzani, C. M. Salá, M. G. Drew, S. W. Dent and M. Maestri, *J. Am. Chem. Soc.*, 1997, **119**, 11864; (b) O. Waldmann, J. Hassmann, P. Müller, G. S. Hanan, D. Volkmer, U. S. Schubert and J.-M. Lehn, *Phys. Rev. Lett.*, 1997, **78**, 3390; (c) E. Zahavy and M. A. Fox, *Chem. Eur. J.*, 1998, **4**, 1647; (d) V. Balzani, A. Credi and M. Venturi, *Curr. Opin. Chem. Biol.*, 1997, **1**, 506.
- 5 S. Welter, K. Brunner, J. W. Hofstraat and L. De Cola, *Nature*, 2003, **421**, 54.
- 6 Y. Kim and C. M. Lieber, *Inorg. Chem.*, 1989, **28**, 3990.
- 7 F. Barigelletti, L. Flamigni, V. Balzani, J.-P. Collin, J.-P. Sauvage, A. Sour, E. C. Constable and A. M. W. C. Thompson, *J. Chem. Soc., Chem. Commun.*, 1993, 942.
- 8 (a) M. Haga, M. M. Ali, H. Sato, H. Monojushiro, K. Nozaki and K. Kano, *Inorg. Chem.*, 1998, **37**, 2320; (b) M. A. Haga, M. Ishizuya, T. Kanesugi, T. Yubaka, D. Sakiyama, J. Fees and W. Kaim, *Indian J. Chem., Sect. A*, 2003, **42**, 2290; (c) M. Haga, T. Takasugi, A. Tomie, M. Ishizuga, T. Yamada, M. D. Hossain and M. Inoue, *Dalton Trans.*, 2003, 2069; (d) M. D. Hossain, M. Haga, B. Gholamkhash, K. Nozaki, M. Tsushima, N. Ikeda and T. Ohno, *Collect. Czech. Chem. Commun.*, 2001, **66**, 307; (e) M. D. Hossain, R. Ueno and M. Haga, *Inorg. Chem. Commun.*, 2000, **3**, 35; (f) M. M. Ali, H. Sato, M. A. Haga, K. Tanaka, A. Yoshimura and T. Ohno, *Inorg. Chem.*, 1998, **37**, 6176.
- 9 (a) R. Hage, J. G. Haasnoot, H. A. Nieuwenhuis, J. Reedijk, D. J. A. De Ridder and J. G. Vos, *J. Am. Chem. Soc.*, 1990, **112**, 9245; (b) P. Passaniti, W. R. Browne, F. C. Lynch, D. Hughes, M. Nieuwenhuyzen, P. James, M. Maestri and J. G. Vos, *J. Chem. Soc., Dalton Trans.*, 2002, 1740; (c) W. R. Browne, F. Weldon, A. L. Guckian and J. G. Vos, *Collect. Czech. Chem. Commun.*, 2003, **68**, 1467; (d) W. R. Browne, C. M. O'Connor, C. Villani and J. G. Vos, *Inorg. Chem.*, 2001, **40**, 5461.
- 10 (a) C. H. Braunstein, A. D. Baker, T. C. Streckas and H. D. Gafney, *Inorg. Chem.*, 1984, **23**, 857; (b) Y. Fuchs, S. Lofters, T. Dieter, W. Shi, R. Morgan, T. C. Streckas, H. D. Gafney and A. D. Baker, *J. Am. Chem. Soc.*, 1987, **109**, 2691; (c) W. R. Murphy, K. J. Brewer, G. Gettliffe and J. D. Petersen, *Inorg. Chem.*, 1989, **28**, 81; (d) K. Kalyanasundaram and Md. K. Nazeeruddin, *Inorg. Chem.*, 1990, **29**, 1888; (e) R. M. Berger, *Inorg. Chem.*, 1990, **29**, 1920; (f) G. Denti, S. Campagna, L. Sabatino, S. Serroni, M. Ciano and V. Balzani, *Inorg. Chem.*, 1990, **29**, 4750.
- 11 C. Creutz, *Prog. Inorg. Chem.*, 1963, **30**, 1.
- 12 (a) E. V. Dose and L. J. Wilson, *Inorg. Chem.*, 1978, **17**, 2660; (b) R. Sahai, D. P. Rillema, R. Shaver, S. van Wallendaal, D. C. Jackman and M. Boldaji, *Inorg. Chem.*, 1989, **28**, 1022.
- 13 (a) W. Kaim, *Coord. Chem. Rev.*, 2002, **230**, 127; (b) W. Kaim, A. Klein and M. Glöckle, *Acc. Chem. Res.*, 2000, **33**, 755; (c) B. Sarker, W. Kaim, A. Klein, B. Schwederski, J. Fiedler, C. Duboc-Toia and G. K. Lahiri, *Inorg. Chem.*, 2003, **42**, 6172.
- 14 (a) J. M. de Wolf, R. Hage, J. G. Haasnoot, J. Reedijk and J. G. Vos, *New J. Chem.*, 1991, **15**, 501; (b) H. E. B. Lempers, J. G. Haasnoot, J. Reedijk, R. Hage, F. Weldon and J. G. Vos, *Inorg. Chim. Acta.*, 1994, **225**, 67; (c) F. Barigelletti, L. Flamigni, V. Balzani, J.-P. Collin, J. P. Sauvage, A. Sour, E. C. Constable and A. M. W. Cargill Thompson, *J. Am. Chem. Soc.*, 1994, **116**, 7692; (d) M. T. Indelli, F. Scandola, J.-P. Collin, J.-P. Sauvage and A. Sour, *Inorg. Chem.*, 1996, **35**, 303; T. Ohno, K. Nozaki and M. Haga, *Inorg. Chem.*, 1992, **31**, 4256; (e) M. Haga, M. M. Ali, S. Koseki, K. Fujimoto, A. Yoshimura, K. Nozaki, T. Ohno, K. Nakajima and D. J. Stufkens, *Inorg. Chem.*, 1996, **35**, 3335; (f) D. P. Rillema, R. Sahai, P. Matthews, A. K. Edwards, R. J. Shaver and L. Morgan, *Inorg. Chem.*, 1990, **29**, 167.
- 15 B. P. Sullivan, D. J. Salmon and T. J. Meyer, *Inorg. Chem.*, 1978, **17**, 3334.
- 16 D. A. Buckingham, F. P. Dwyer, H. A. Goodwin and A. M. Sargeson, *Aust. J. Chem.*, 1964, **17**, 325.
- 17 G. M. Sheldrick, *SHELX-97*, Universität Göttingen, 1997.
- 18 W. R. Heineman, *J. Chem. Educ.*, 1983, **60**, 4.
- 19 J. P. Chang, E. Y. Fung and J. C. Curtis, *Inorg. Chem.*, 1986, **25**, 4233.
- 20 N. G. Connelly and W. E. Geiger, *Chem. Rev.*, 1996, **96**, 877.
- 21 D. S. Jones, A. F. Brown, A. D. Woolfson, A. C. Dennis, L. J. Matchett and S. E. J. Bell, *J. Pharm. Sci.*, 2000, **89**, 563–571.
- 22 (a) C. G. Coates, L. Jacquet, J. J. McGarvey, S. E. J. Bell, A. H. R. Al-Obaidi and J. M. Kelly, *J. Am. Chem. Soc.*, 1997, **119**, 7130; (b) C. G. Coates, J. Olofsson, M. Coletti, J. J. McGarvey, B. Onfelt, P. Lincoln, B. Norden, E. Tuite, P. Matousek and A. W. Parker, *J. Phys. Chem. B*, 2001, **105**, 12653–12664.
- 23 *Gaussian 03, Revision B 04*, M. J. Frisch, G. W. Trucks, H. B. Schlegel, G. E. Scuseria, M. A. Robb, J. R. Cheeseman, J. A. Montgomery, Jr., T. Vreven, K. N. Kudin, J. C. Burant, J. M. Millam, S. S. Iyengar, J. Tomasi, V. Barone, B. Mennucci, M. Cossi, G. Scalmani, N. Rega, G. A. Petersson, H. Nakatsuji, M. Hada, M. Ehara, K. Toyota, R. Fukuda, J. Hasegawa, M. Ishida, T. Nakajima, Y. Honda, O. Kitao, H. Nakai, M. Klene, X. Li, J. E. Knox, H. P. Hratchian, J. B. Cross, C. Adamo, J. Jaramillo, R. Gomperts, R. E. Stratmann, O. Yazyev, A. J. Austin, R. Cammi, C. Pomelli, J. W. Ochterski, P. Y. Ayala, K. Morokuma, G. A. Voth, P. Salvador, J. J. Dannenberg, V. G. Zakrzewski, S. Dapprich, A. D. Daniels, M. C. Strain, O. Farkas, D. K. Malick, A. D. Rabuck, K. Raghavachari, J. B. Foresman, J. V. Ortiz, Q. Cui, A. G. Baboul, S. Clifford, J. Cioslowski, B. B. Stefanov, G. Liu, A. Liashenko, P. Piskorz, I. Komaromi, R. L. Martin, D. J. Fox, T. Keith, M. A. Al-Laham, C. Y. Peng, A. Nanayakkara, M. Challacombe, P. M. W. Gill, B. Johnson, W. Chen, M. W. Wong, C. Gonzalez, and J. A. Pople, Gaussian, Inc., Pittsburgh PA, 2003.
- 24 A. D. Becke, *J. Chem. Phys.*, 1993, **98**, 5648.
- 25 C. Lee, W. Yang and R. G. Parr, *Phys. Rev. B*, 1988, **37**, 785.
- 26 (a) T. H. Dunning, Jr. and P. J. Hay, in *Modern Theoretical Chemistry*, ed. H. F. Schaefer III, Plenum, New York, 1976, vol. 3, p. 1; (b) P. J. Hay and W. R. Wadt, *J. Chem. Phys.*, 1985, **82**, 270; (c) P. J. Hay and W. R. Wadt, *J. Chem. Phys.*, 1985, **82**, 284; (d) P. J. Hay and W. R. Wadt, *J. Chem. Phys.*, 1985, **82**, 299.
- 27 N. M. O'Boyle and J. G. Vos, *Gauss Sum 0.8*, Dublin City University, 2004. Available at <http://gausssum.sourceforge.net>.
- 28 (a) R. Hage, J. G. Haasnoot, J. Reedijk, R. Wang, E. M. Ryan, J. G. Vos, A. L. Spek and A. J. M. Duisenberg, *Inorg. Chim. Acta*, 1990, **174**, 77; (b) D. P. Rillema, D. S. Jones, C. Woods and H. A. Levy, *Inorg. Chem.*, 1992, **31**, 2935; (c) R. Hage, J. P. Turkenburg, R. A. G. de Graaf, J. G. Haasnoot, J. Reedijk and J. G. Vos, *Acta Crystallogr., Sect. C*, 1980, **45**, 381; (d) D. P. Rillema, D. S. Jones and H. A. Levy, *J. Chem. Soc., Chem. Commun.*, 1979, 849.
- 29 F. Weldon, L. Hammarström, E. Mukhtar, R. Hage, E. Gunneweg, J. G. Haasnoot, J. Reedijk, W. R. Browne, A. L. Guckian and J. G. Vos, *Inorg. Chem.*, 2004, **43**, 4471.
- 30 W. R. Browne, C. M. O'Connor, H. P. Hughes, R. Hage, O. Walter, M. Doering, J. F. Gallagher and J. G. Vos, *J. Chem. Soc., Dalton Trans.*, 2002, 4048.
- 31 (a) W. J. Vining, J. V. Caspar and T. J. Meyer, *J. Phys. Chem.*, 1985, **89**, 1095; (b) M. Wrighton and D. L. Morse, *J. Am. Chem. Soc.*, 1974, **96**, 996; (c) A. Juris, V. Balzani, F. Barigelletti, S. Campagna, P. Belser and A. von Zelewsky, *Coord. Chem. Rev.*, 1988, **84**, 85.
- 32 S. Fanni, F. Weldon, L. Hammarström, E. Mukhtar, W. R. Browne, T. E. Keyes and J. G. Vos, *Eur. J. Inorg. Chem.*, 2001, 529.
- 33 W. R. Browne and J. G. Vos, *Coord. Chem. Rev.*, 2001, **219**, 761, and references therein.
- 34 (a) K. Maruszewski, K. Bajdor, D. P. Strommen and J. R. Kincaid, *J. Phys. Chem.*, 1995, **99**, 6286; (b) P. K. Mallick, G. D. Danzer, D. P. Strommen and J. R. Kincaid, *J. Phys. Chem.*, 1988, **92**, 5628; (c) D. P. Strommen, P. K. Mallick, G. D. Danzer and R. S. Lumpkin, *J. Phys. Chem.*, 1990, **94**, 1357.
- 35 (a) A. C. Ribou, J.-P. Launay, K. Takahashi, T. Nihira, S. Tarutani and C. W. Spangler, *Inorg. Chem.*, 1994, **33**, 1325; (b) P. Laine, V. Marvaud, A. Gourdon, J.-P. Launay, M. L. Sachtleben, H. Li and C. W. Spangler, *Inorg. Chem.*, 1996, **35**, 3735.
- 36 E. Krausz, G. Moran and H. Riesen, *Chem. Phys. Lett.*, 1990, **165**, 401.
- 37 E. M. Kober, B. P. Sullivan, W. J. Dressick, J. V. Caspar and T. J. Meyer, *J. Am. Chem. Soc.*, 1980, **102**, 7385.
- 38 D. E. Richardson and H. Taube, *Inorg. Chem.*, 1981, **20**, 1278.
- 39 S. I. Gorelsky and A. B. P. Lever, *J. Organomet. Chem.*, 2001, **635**, 187.
- 40 This representation gives a better overview of the nature of the frontier orbitals, especially where neighbouring orbitals are closely-spaced.